ASSIGNMENT 3

Yash Khobragade

May 3, 2025

1 Problem Statement

The lid-driven cavity flow is a benchmark problem in computational fluid dynamics that involves a square cavity filled with fluid, where the top wall (lid) moves at a constant velocity while the other walls remain stationary. This creates a recirculating flow pattern inside the cavity.

1.1 Problem Specifications

The problem is defined as follows:

- Cavity dimensions: 40×40 cm
- Fluid properties: Constant density, kinematic viscosity ($\nu = \mu/\rho$) of 0.004 m^2/s
- Uniform grid: $\Delta x = \Delta y = 0.005$ m (80×80 cells)
- Boundary conditions:
  - Top wall (lid): Moving with velocity $U_{lid} = 1$ m/s in the positive x-direction
  - Bottom, left, and right walls: No-slip condition & No penetration condition (u = v =0)
- Convergence criterion: 10^{-5} for the mass source

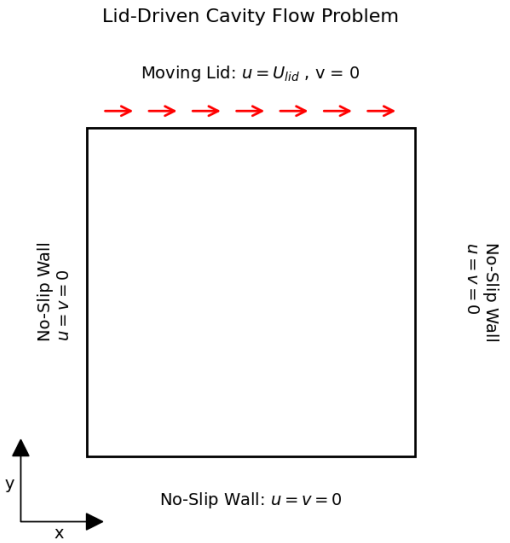

Figure 1: Problem schematic

1.2 Governing Equations

The flow in this case is governed by the incompressible Navier-Stokes equations under steady state conditions:
Continuity equation

$$\frac{\partial(\rho u)}{\partial x} + \frac{\partial(\rho v)}{\partial x} = 0 \tag{1}$$

x - momentum equation

$$\rho(u\frac{\partial u}{\partial x} + v\frac{\partial u}{\partial y}) = -\frac{\partial P}{\partial x} + \mu(\frac{\partial^2 u}{\partial x^2} + \frac{\partial^2 u}{\partial y^2}) \tag{2}$$

y - momentum equation

$$\rho(u\frac{\partial v}{\partial x} + v\frac{\partial v}{\partial y}) = -\frac{\partial P}{\partial y} + \mu(\frac{\partial^2 v}{\partial x^2} + \frac{\partial^2 v}{\partial y^2}) \tag{3}$$

where $\mathbf{u}$ and $\mathbf{v}$ are the velocity vectors, P is the pressure, ρ is the density, and μ is the dynamic viscosity.

2 Grid Arrangement

2.1 Staggered Grid

A staggered grid arrangement is used to avoid the checkerboard pressure field issue that can occur with collocated grids. In the staggered grid:

- Pressure (p) is stored at cell centers
- u-velocity components are stored at the east cell faces
- v-velocity components are stored at the north faces

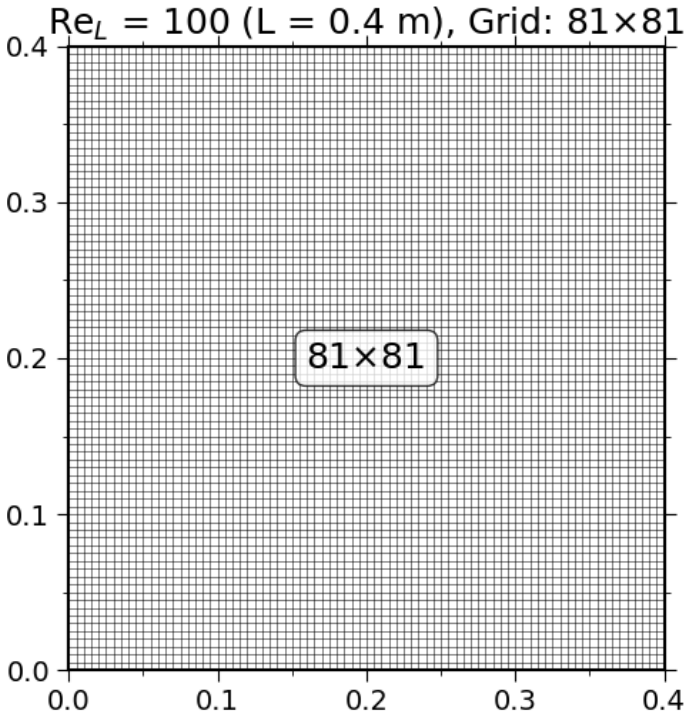

Figure 2: Uniform grid arrangement with $\Delta x = \Delta y = 0.005m$

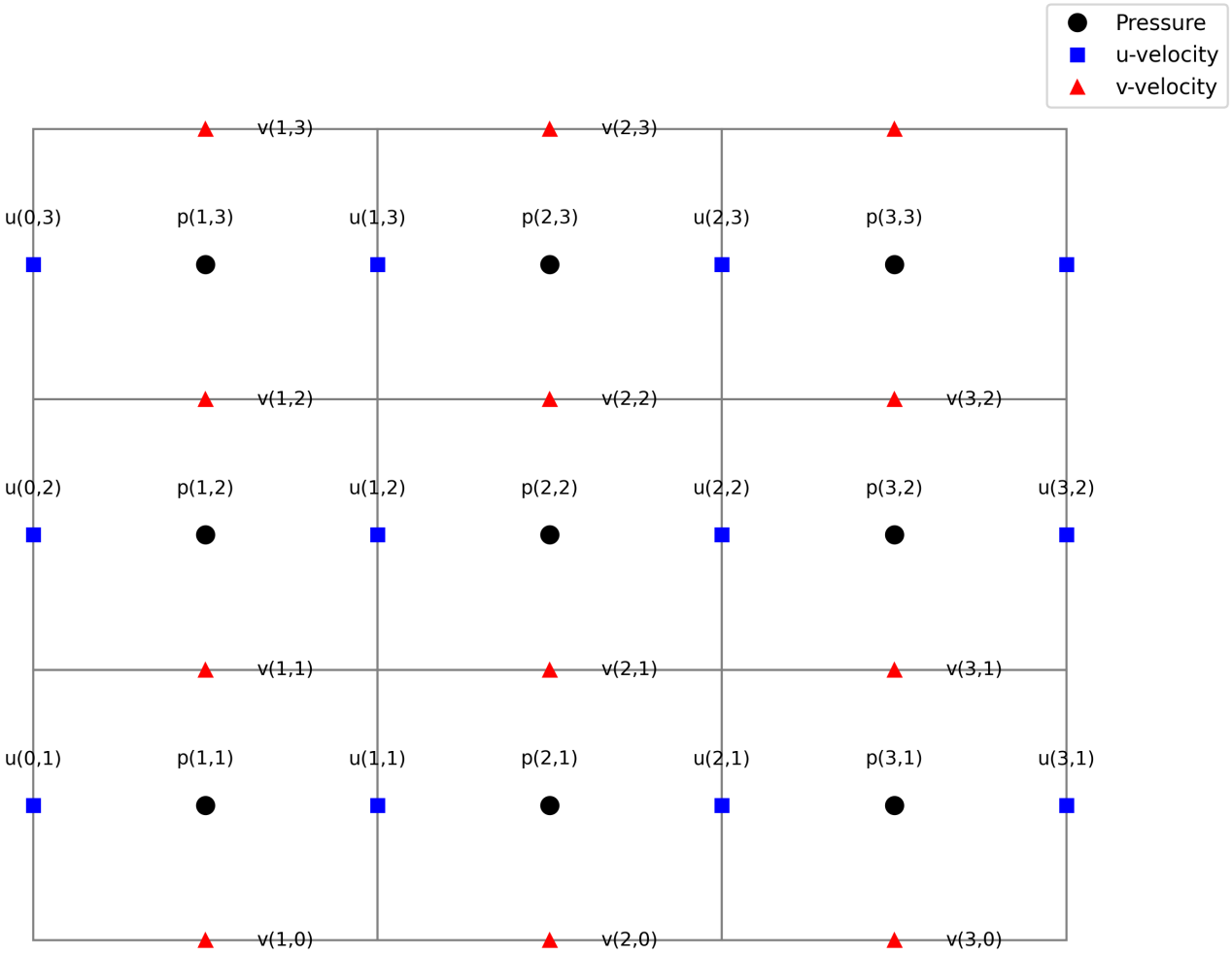

Figure 3: Staggered grid arrangement showing the locations of pressure (p), u-velocity, and v-velocity.

2.2 Grid Indexing

The grid consists of 80×80 cells, with indices running from 1 to 80 in both directions. Additional cells are added at the boundaries to handle boundary conditions:

- Pressure grid: $(nx + 1) \times (ny + 1)$ cells
- u-velocity grid: $(nx + 1) \times (ny + 2)$ cells
- v-velocity grid: $(nx + 2) \times (ny + 1)$ cells

where $nx = ny = 80$ are the number of cells in the x and y directions. I've also taken ghost cell faces into account while getting the cells for staggered grid

3 Discretization & SIMPLE Algorithm

3.1 Finite Volume Method

The Finite Volume Method (FVM) is used to discretize the governing equations. The domain is divided into a finite number of control volumes, and the governing equations are solved on each CV. The fluxes across the control volume faces are approximated using different discretization schemes.

Now we will start with Discretization of x-momentum equation, also note that I'll be using Primitive variable based solution approach.

$$\int_s^n \int_w^e \frac{u\,\partial(\rho u)}{\partial x}\,dx\,dy + \int_w^e \int_s^n \frac{v\,\partial(\rho u)}{\partial y}\,dy\,dx \;=\; \int_s^n \int_w^e \left[\frac{\partial}{\partial x}\left(\mu\frac{\partial u}{\partial x}\right)\right]dx\,dy + \int_w^e \int_s^n \left[\frac{\partial}{\partial y}\left(\mu\frac{\partial u}{\partial y}\right)\right]dy\,dx - \int_s^n \int_w^e \frac{\partial p}{\partial x}\,dx\,dy$$

$$u_e(\rho u)_e\Delta y - u_w(\rho u)_w\Delta y + u_n(\rho u)_n\Delta x - u_s(\rho u)_s\Delta x \;=\; (p_P - p_E)\Delta y + \mu\left(\frac{\partial u}{\partial y}\right)_e\Delta y - \mu\left(\frac{\partial u}{\partial y}\right)_w\Delta y + \mu\left(\frac{\partial u}{\partial x}\right)_n\Delta x - \mu\left(\frac{\partial u}{\partial x}\right)_s\Delta x$$

Using CDS scheme

$$(\rho u)_e\frac{(u_E+u_P)}{2}\Delta y - (\rho u)_w\frac{(u_P+u_W)}{2}\Delta y + (\rho u)_n\frac{(u_P+u_N)}{2}\Delta x - (\rho u)_s\frac{(u_P+u_S)}{2}\Delta x \;=\; (p_P - p_E)\Delta y + \mu\left(\frac{u_E-u_P}{(\delta x)_e}\right)\Delta y - \mu\left(\frac{u_P-u_W}{(\delta x)_w}\right)\Delta y + \mu\left(\frac{u_N-u_P}{(\delta y)_n}\right)\Delta x - \mu\left(\frac{u_P-u_S}{(\delta y)_s}\right)\Delta x$$

As our problem states use of uniform grid,

$$(\delta x)_e = (\delta x)_s = \Delta x$$
$$(\delta y)_n = (\delta y)_s = \Delta y$$

We will substitute the above relation in our discretized equation, we will also rearrange our equation

$$u_P\left(\frac{\rho u_e}{2}\Delta y - \frac{\rho u_w}{2}\Delta y + \frac{\rho u_n}{2}\Delta x - \frac{\rho u_s}{2}\Delta x + \frac{2\mu\Delta y}{\Delta x} + \frac{2\mu\Delta x}{\Delta y}\right) = u_E\left(-\frac{\rho u_e}{2}\Delta y + \frac{\mu\Delta y}{\Delta x}\right) + u_W\left(\frac{\rho u_w}{2}\Delta y + \frac{\mu\Delta y}{\Delta x}\right) + u_N\left(\frac{\rho u_n}{2}\Delta x + \frac{\mu\Delta x}{\Delta y}\right) + u_S\left(-\frac{\rho u_s}{2}\Delta x + \frac{\mu\Delta x}{\Delta y}\right) + (p_P - p_E)\Delta y$$

We can rewrite this as:

$$a_P u_P = a_E u_E + a_W u_W + a_N u_N + a_S u_S + (p_P - p_E)\Delta y$$

where

$$a_E = -\frac{(\rho u)_e\Delta y}{2} + \mu\frac{\Delta y}{\Delta x} \qquad a_W = \frac{(\rho u)_w\Delta y}{2} + \mu\frac{\Delta y}{\Delta x}$$
$$a_N = -\frac{(\rho u)_n\Delta x}{2} + \mu\frac{\Delta x}{\Delta y} \qquad a_S = \frac{(\rho u)_s\Delta x}{2} + \mu\frac{\Delta x}{\Delta y}$$

And

$$a_P = a_E + a_W + a_N + a_S + \left(\frac{(\rho u)_e \Delta y}{2} - \frac{(\rho u)_w \Delta y}{2} + \frac{(\rho u)_n \Delta x}{2} - \frac{(\rho u)_s \Delta x}{2} \right)$$

Remember! u is being calculated on the **east** face.

Thus, we will just change the naming:

$$a_{e,u} = a_E + a_W + a_N + a_S + \left(\frac{(\rho u)_e \Delta y}{2} - \frac{(\rho u)_w \Delta y}{2} + \frac{(\rho u)_n \Delta x}{2} - \frac{(\rho u)_s \Delta x}{2} \right)$$

Here, E, W, N, S refer to the East, South, North, and South postions with respect to the east face that are at Δx and Δy distance from the east face in x and y direction respectively.

Similarly e, w, n, s refer to the east, south, north and south faces with respect to the east face that are at $\Delta x/2$ and $\Delta y/2$ distance from the east face in x and y direction respectively.

Thus,

$$a_{e,u} u_e = a_E u_E + a_W u_W + a_N u_N + a_S u_S + (p_P - p_E)\Delta y$$

Similarly, following this process for the v-momentum equation, we have:

$$a_{e,v} v_n = a_E v_E + a_W v_W + a_N v_N + a_S v_S + (p_P - p_N)\Delta x$$

Here, v is calculated on the north face.

where

$$a_E = -\frac{(\rho u)_e \Delta x}{2} + \mu \frac{\Delta x}{\Delta y} \qquad a_W = \frac{(\rho u)_w \Delta x}{2} + \mu \frac{\Delta x}{\Delta y}$$
$$a_N = -\frac{(\rho u)_n \Delta y}{2} + \mu \frac{\Delta y}{\Delta x} \qquad a_S = \frac{(\rho u)_s \Delta y}{2} + \mu \frac{\Delta y}{\Delta x}$$

Thus,

$$a_{e,v} = a_E + a_W + a_N + a_S + \left(\frac{(\rho u)_e \Delta x}{2} - \frac{(\rho u)_w \Delta x}{2} + \frac{(\rho u)_n \Delta y}{2} - \frac{(\rho u)_s \Delta y}{2} \right)$$

Again, here E, W, N, S and e, w, n, s meaning has changed, please follow what I've mentioned above.

Using UPWIND scheme

The equation form will remain the same,

$$a_{e,u} u_e = a_E u_E + a_W u_W + a_N u_N + a_S u_S + (p_P - p_E)\Delta y$$

only the coefficients will change, because the convective flux that we approximated using CDS in previous scheme has now changed, now: if $u_e > 0$ then

$$u_e = u_P$$

In upwind we approximate the flux from only the upstream component. The revised coefficients for x - momentum equation are:

$$a_E = \mu\frac{\Delta y}{\Delta x} \qquad a_W = (\rho u)_w\Delta y + \mu\frac{\Delta y}{\Delta x}$$
$$a_N = \mu\frac{\Delta x}{\Delta y} \qquad a_S = (\rho u)_s\Delta x + \mu\frac{\Delta x}{\Delta y}$$

And

$$a_{e,u} = a_E + a_W + a_N + a_S + \left(\frac{(\rho u)_e\Delta y}{2} - \frac{(\rho u)_w\Delta y}{2} + \frac{(\rho u)_n\Delta x}{2} - \frac{(\rho u)_s\Delta x}{2}\right)$$

Coefficients for y - momentum equation using upwind scheme are:

$$a_E = \mu\frac{\Delta y}{\Delta x} \qquad a_W = (\rho u)_w\Delta x + \mu\frac{\Delta y}{\Delta x}$$
$$a_N = \mu\frac{\Delta x}{\Delta y} \qquad a_S = (\rho u)_s\Delta y + \mu\frac{\Delta x}{\Delta y}$$

And

$$a_{e,v} = a_E + a_W + a_N + a_S + \left(\frac{(\rho u)_e\Delta x}{2} - \frac{(\rho u)_w\Delta x}{2} + \frac{(\rho u)_n\Delta y}{2} - \frac{(\rho u)_s\Delta y}{2}\right)$$

Using Hybrid scheme

Again the equation will be same, only coefficients will change: for x - momentum equation :

$$a_E = \begin{cases} \mu\frac{\Delta y}{\Delta x} - (\rho u)_e\Delta y, & \mathrm{Pe}_e < -2, \\ -\frac{(\rho u)_e\Delta y}{2} + \mu\frac{\Delta y}{\Delta x}, & -2 \le \mathrm{Pe}_e \le 2, \\ \mu\frac{\Delta y}{\Delta x}, & \mathrm{Pe}_e > 2, \end{cases} \quad a_W = \begin{cases} \mu\frac{\Delta y}{\Delta x}, & \mathrm{Pe}_w < -2, \\ \frac{(\rho u)_w\Delta y}{2} + \mu\frac{\Delta y}{\Delta x}, & -2 \le \mathrm{Pe}_w \le 2, \\ (\rho u)_w\Delta y + \mu\frac{\Delta y}{\Delta x}, & \mathrm{Pe}_w > 2, \end{cases}$$

$$a_N = \begin{cases} \mu\frac{\Delta x}{\Delta y} - (\rho v)_n\Delta x, & \mathrm{Pe}_n < -2, \\ -\frac{(\rho v)_n\Delta x}{2} + \mu\frac{\Delta x}{\Delta y}, & -2 \le \mathrm{Pe}_n \le 2, \\ \mu\frac{\Delta x}{\Delta y}, & \mathrm{Pe}_n > 2, \end{cases} \quad a_S = \begin{cases} \mu\frac{\Delta x}{\Delta y}, & \mathrm{Pe}_s < -2, \\ \frac{(\rho v)_s\Delta x}{2} + \mu\frac{\Delta x}{\Delta y}, & -2 \le \mathrm{Pe}_s \le 2, \\ (\rho v)_s\Delta x + \mu\frac{\Delta x}{\Delta y}, & \mathrm{Pe}_w > 2, \end{cases}$$

and

$$a_{e,u} = a_E + a_W + a_N + a_S + \left(\frac{(\rho u)_e\Delta y}{2} - \frac{(\rho u)_w\Delta y}{2} + \frac{(\rho u)_n\Delta x}{2} - \frac{(\rho u)_s\Delta x}{2}\right)$$

For y - momentum equation we have the coefficients:

$$a_E = \begin{cases} \mu\frac{\Delta x}{\Delta y} - (\rho u)_e\Delta x, & \mathrm{Pe}_e < -2, \\ -\frac{(\rho u)_e\Delta x}{2} + \mu\frac{\Delta x}{\Delta y}, & -2 \le \mathrm{Pe}_e \le 2, \\ \mu\frac{\Delta x}{\Delta y}, & \mathrm{Pe}_e > 2, \end{cases} \quad a_W = \begin{cases} \mu\frac{\Delta x}{\Delta y}, & \mathrm{Pe}_w < -2, \\ \frac{(\rho u)_w\Delta x}{2} + \mu\frac{\Delta x}{\Delta y}, & -2 \le \mathrm{Pe}_w \le 2, \\ (\rho u)_w\Delta x + \mu\frac{\Delta x}{\Delta y}, & \mathrm{Pe}_w > 2, \end{cases}$$

$$a_N = \begin{cases} \mu\frac{\Delta y}{\Delta x} - (\rho v)_n \Delta y, & \text{Pe}_n < -2, \\ -\frac{(\rho v)_n \Delta y}{2} + \mu\frac{\Delta y}{\Delta x}, & -2 \le \text{Pe}_n \le 2, \\ \mu\frac{\Delta y}{\Delta x}, & \text{Pe}_n > 2, \end{cases} \quad a_S = \begin{cases} \mu\frac{\Delta y}{\Delta x}, & \text{Pe}_s < -2, \\ \frac{(\rho v)_s \Delta y}{2} + \mu\frac{\Delta y}{\Delta x}, & -2 \le \text{Pe}_s \le 2, \\ (\rho v)_s \Delta y + \mu\frac{\Delta y}{\Delta x}, & \text{Pe}_w > 2, \end{cases}$$

and

$$a_{e,v} = a_E + a_W + a_N + a_S + \left(\frac{(\rho u)_e \Delta x}{2} - \frac{(\rho u)_w \Delta x}{2} + \frac{(\rho u)_n \Delta y}{2} - \frac{(\rho u)_s \Delta y}{2} \right)$$

Now we have coefficients of all the schemes. We need to devise a algorithm such that we can take care of the pressure term and get a converged solution.

Next steps are going to be the same for every scheme.

We will use generalized form of discretized momentum equation. The x-momentum equation in generalized Discretized form is:

$$a_e u_e = \sum a_{nb} u_{nb} + b + (P_P - P_E) A_e \quad (1)$$

This uses a staggered CV for u velocity. The figure at the start shows how u velocity will be stored

- $a_{nb} \rightarrow$ coefficients containing neighbours' combined convection-diffusion influence.
- $b \rightarrow$ source term arising from pressure gradients.
- $u_{nb} \rightarrow$ u velocity, there are 4 neighbours here.
- $A_e = \Delta y \times 1$

Similarly, for the v-momentum equation, we will use a staggered C-V for v velocity.

The generalized Discretized equation for V momentum is :

$$a_n v_n = \sum a_{nb} v_{nb} + b + (P_P - P_N) A_n \quad (2)$$

where $A_n = \Delta x \times 1$.

We know, the momentum equation can be solved only when the pressure field is given or is somehow estimated. We will guess the pressure field$\rightarrow P^*$.

We will get an imperfect velocity field u^*, v^* based on our guessed pressure field. The guessed velocity field can be solved using the following Discretized equations:

$$a_e u_e^* = \sum a_{nb} u_{nb}^* + b + (P_P^* - P_E^*) A_e \quad (3)$$
$$a_n v_n^* = \sum a_{nb} v_{nb}^* + b + (P_P^* - P_N^*) A_n \quad (4)$$

The above equations solve for guessed velocity. We still need to correct it!. We will introduce **pressure & velocity corrections**.

We can write the correct pressure field as:

$$P = P^* + P' \quad (5)$$

where P' represents pressure corrections.

Similarly, for velocity corrections:

$$u = u^* + u' \quad (6)$$
$$v = v^* + v' \quad (7)$$

where u' and v' are velocity corrections.

Subtracting equation (3) from (1), we get:

$$a_c u'_e = \sum a_{nb} u'_{nb} + (P'_P - P'_E) A_e \quad (8)$$

We will drop these terms ($\sum a_{nb} u'_{nb}$) in our correction calculations.

Therefore:

$$a_c u'_e = (P'_P - P'_E) A_e \quad (9)$$

This gives the velocity correction equation :

$$u'_e = \frac{A_e}{a_c}(P'_P - P'_E) \quad (10)$$

where $d_e = A_e/a_e$.

From equation (6), we can write:

$$u_e = u^*_e + d_e(P'_P - P'_E) \quad (11)$$

Similarly for v :

$$v_n = v^*_n + d_n(P'_P - P'_N) \quad (12)$$

We got our velocity correction equations!.

Now we need a pressure correction equation. Upto now we were using staggered grids for u & v velocity . For P, we will store P in the main CV. In the figure at the start I've shown where we will store P

To get the pressure correction equation, we will integrate continuity over the main CV.

The integral form of the continuity equation over a control volume is shown, indicating fluxes across faces:

$$\int_s^n \int_w^e \left(\frac{\partial(\rho u)}{\partial x} + \frac{\partial(\rho v)}{\partial y} \right) dxdy = (\rho u)_e \Delta y - (\rho u)_w \Delta y + (\rho v)_n \Delta x - (\rho v)_s \Delta x$$

We will use values of u_e, u_w, u_n & u_s from equations (11) & (12). We will eventually get an equation:

$$a_P P' = a_E P'_E + a_W P'_W + a_N P'_N + a_S P'_S + b \quad (13)$$

where the coefficients are:

$$a_E = \rho d_e \Delta y \qquad a_W = \rho d_w \Delta y$$
$$a_N = \rho d_n \Delta x \qquad a_S = \rho d_s \Delta x$$
$$a_P = a_E + a_W + a_N + a_S$$

and the source term b is:

$$b = \rho(u_w^* \Delta y - u_e^* \Delta y) + \rho(v_s^* \Delta x - v_n^* \Delta x)$$

We've got everything we need now. Next what we can do is arrange everything step by step and make it into a Algorithm

3.2 SIMPLE Algorithm

The SIMPLE (Semi-Implicit Method for Pressure-Linked Equations) algorithm is used to handle the pressure-velocity coupling. The algorithm consists of the following steps:

Algorithm 1 SIMPLE Algorithm

1: Initialize pressure field (Guess the pressure field P^*)
2: **while** not converged **do**
3: Solve momentum equations (3) and (4) to obtain u^* and v^*
4: Solve pressure correction equation (13) to obtain P'
5: Correct pressure using equation (5)
6: Correct velocities from equations (11) and (12)
7: Treat the corrected pressure as the new P^*

3.3 Relaxation Factors

Relaxation factors are used to stabilize the iterative process:

$$u = u^* + \alpha_u(u') \tag{4}$$
$$v = v^* + \alpha_v(v') \tag{5}$$
$$p = p + \alpha_p p' \tag{6}$$

where α_u, α_v, and α_p are the relaxation factors for u-velocity, v-velocity, and pressure, respectively.

I will show how the use of different relaxation factors affects the convergence and accurary of our solution in results analysis.

3.4 Boundary Condition Implementation

The boundary conditions are as follows:

- **Lid at top** ($y = 0.4$): u = 1 m/s, v = 0
- **Bottom Wall** ($y = 0$): u = 0, v = 0
- **Left Wall** ($x = 0$): u = 0, v = 0
- **Right Wall** ($x = 0.4$): u = 0, v = 0

Also on the boundary nodes:

$$a_E(nx - 1) = 0$$
$$a_W(0) = 0$$
$$a_N(ny - 1) = 0$$
$$a_S(0) = 0$$

4 Result Analysis

4.1 Convergence Behavior

The convergence behavior of the three discretization schemes is compared in terms of the number of iterations required to reach the convergence criterion and the rate of convergence.

For the data specified in problem statement we get the following convergence graph:

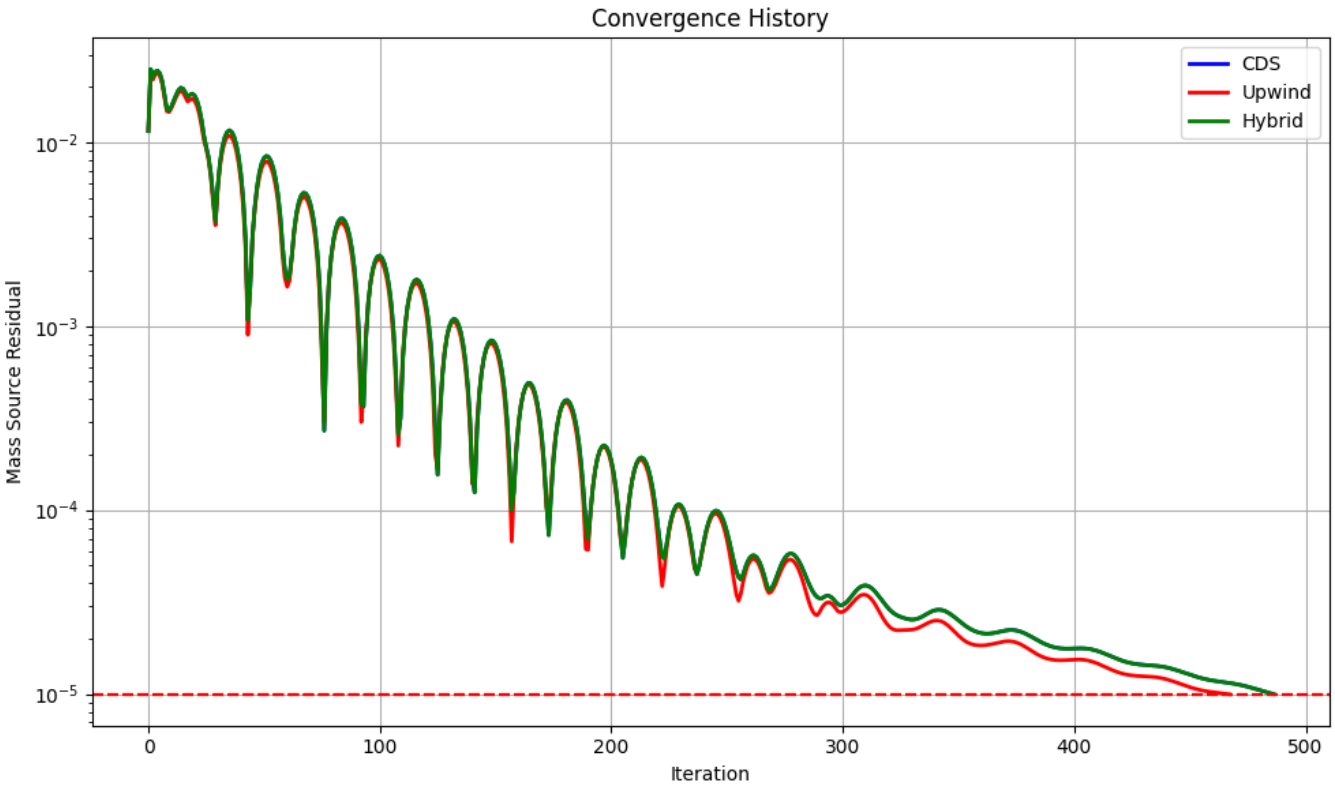

Figure 4: Convergence history of the mass conservation residual for different discretization schemes

The convergence criterion is set at $1e-5$ for the mass source, indicated by a dashed red line on the plot. From this graph, it can be inferred that the Upwind scheme takes less iterations than the CDS and Hybrid schemes. Also as the iterations increase solution becomes more stable.
We can also observe that the hybrid scheme and CDS scheme have the same convergence graph, this is because of the Peclet number being in range -2 to 2.

4.2 Velocity Vectors

The velocity vector plots show the flow pattern in the cavity for each discretization scheme. We might not be able to distinguish much with these plots from our naked eye.

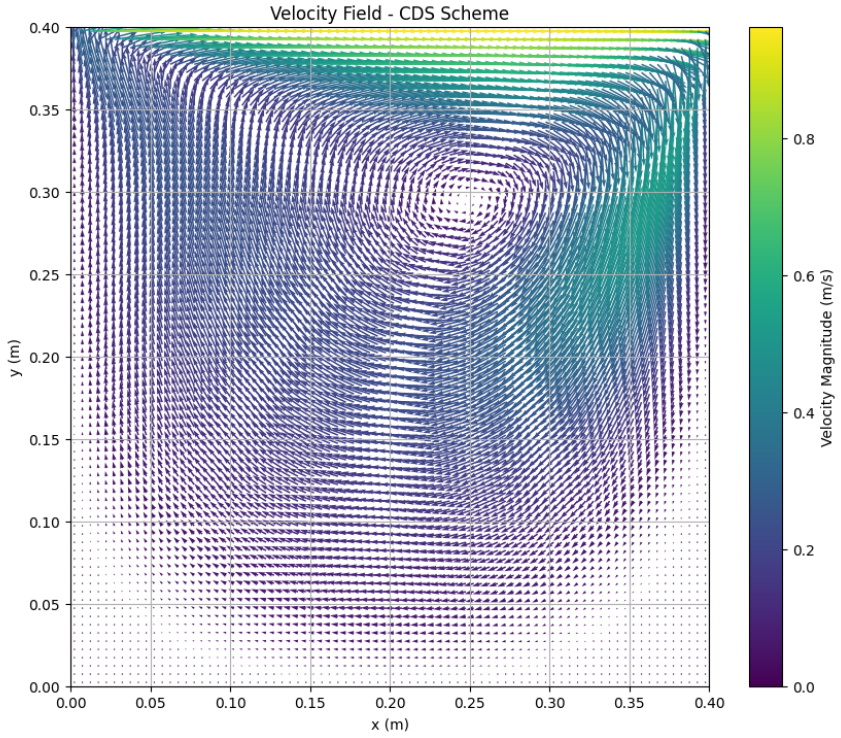

Figure 5: velocity vectors for CDS scheme

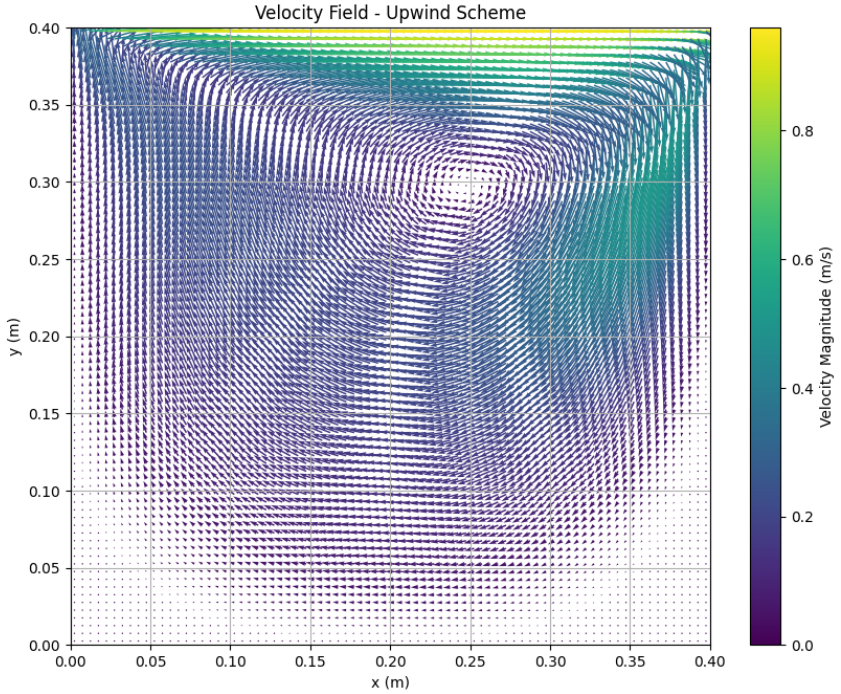

Figure 6: velocity vectors for Upwind scheme

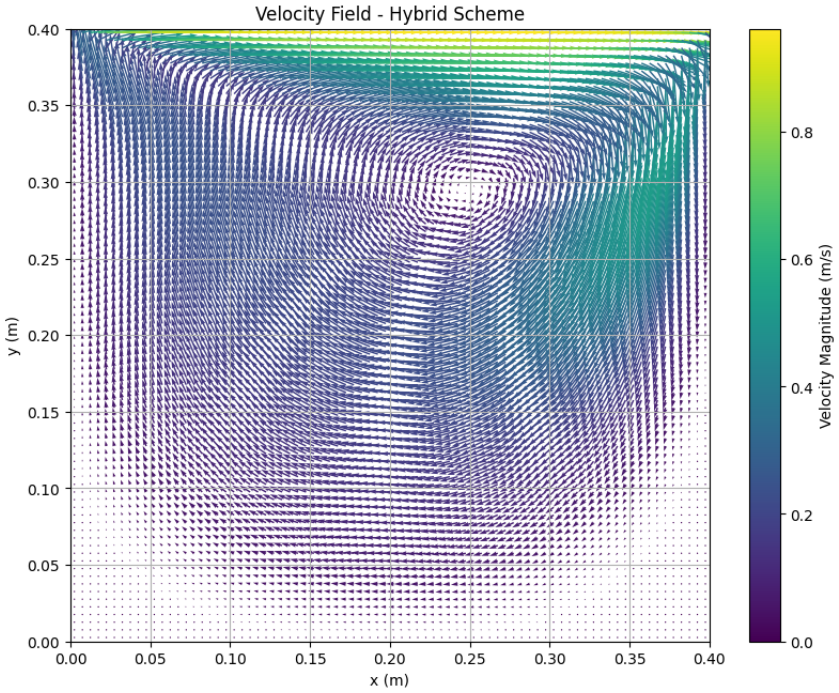

Figure 7: velocity vectors for Hybrid scheme

4.3 Streamline Pattern

The streamline patterns visualize the flow structure, showing the primary vortex and secondary vortices in the corners for each discretization scheme.

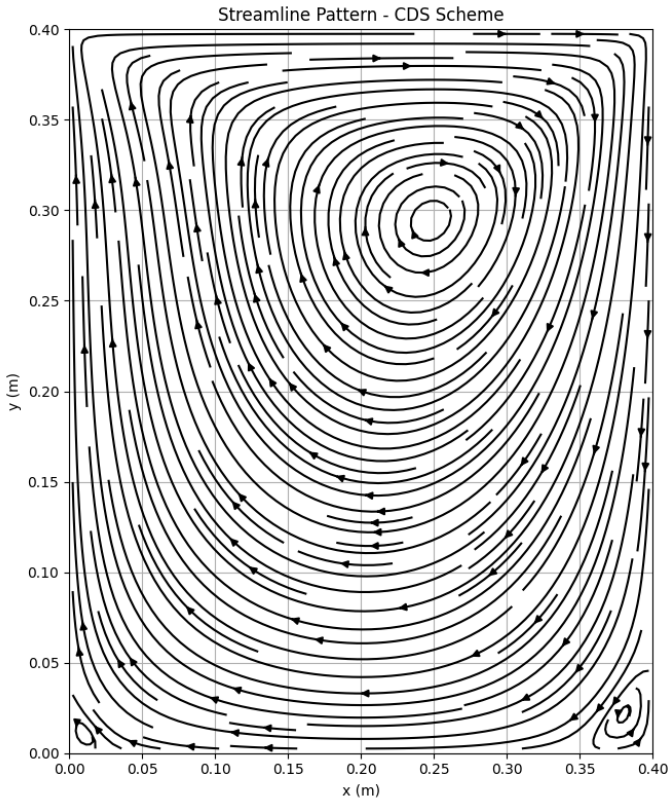

Figure 8: Streamlines for CDS scheme

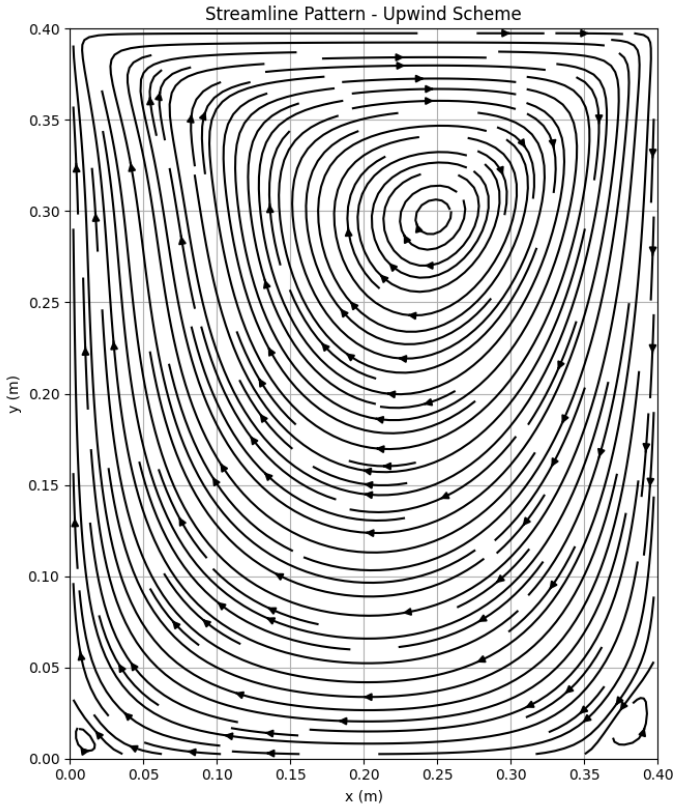

Figure 9: Streamlines for Upwind scheme

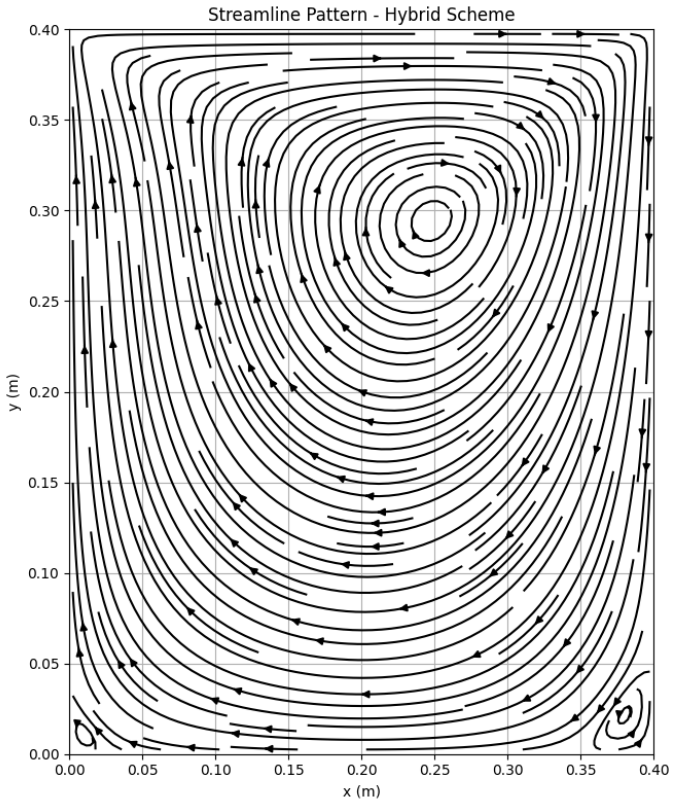

Figure 10: Streamlines for Hybrid scheme

A key feature observed in these plots is the primary vortex in the center of the cavity, driven by

the moving lid at the top. Also, the streamlines show the presence of secondary vortices in the corners of the cavity. We can also identify the difference in secondary vortices between upwind and CDS/Hybrid scheme. Upwind is having difficulty resolving secondary vortices in the corner.

These observed flow patterns are consistent with benchmark results!

4.4 Velocity Profiles

The velocity profiles at the mid-sections of the cavity provide a quantitative comparison between the different discretization schemes. Ghia et al solution is available so i will put that in too.

The difference between these schemes become more apparent at higher Re, therefore I have also plotted the profiles for Re = 400.

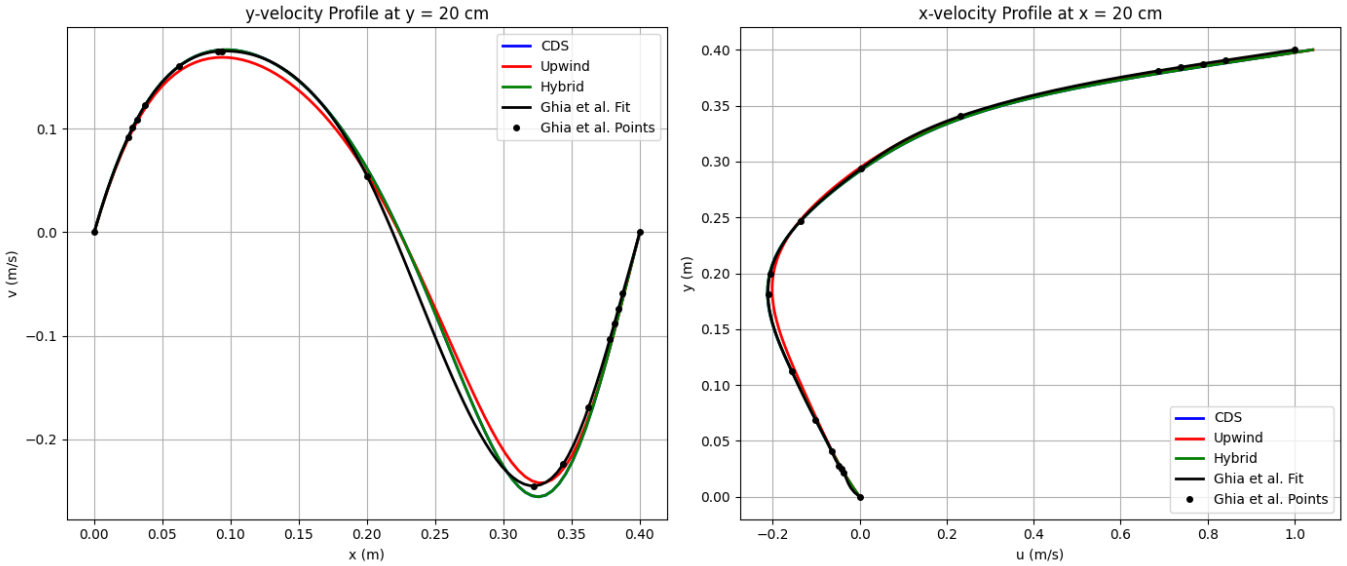

Figure 11: u and v velocity profiles at mid-section for Re = 100

At Re = 100, the profiles for the three schemes appear quite similar .Although the Upwind scheme shows an under and over predictive nature in the velocity profiles compared to the other schemes.

4.5 Comparision of different relaxation factors

Now we'll compare how different relaxation factors affect our convergence and solution accuracy. The relaxation factors are used to stabilize the iterative process. For the above calculation i've used $\alpha_u = \alpha_v = 0.5$ & $\alpha_p = 0.3$. Here we'll go through multiple different arrangements and decide which is the optimal arrangement and what arrangements should be avoid.

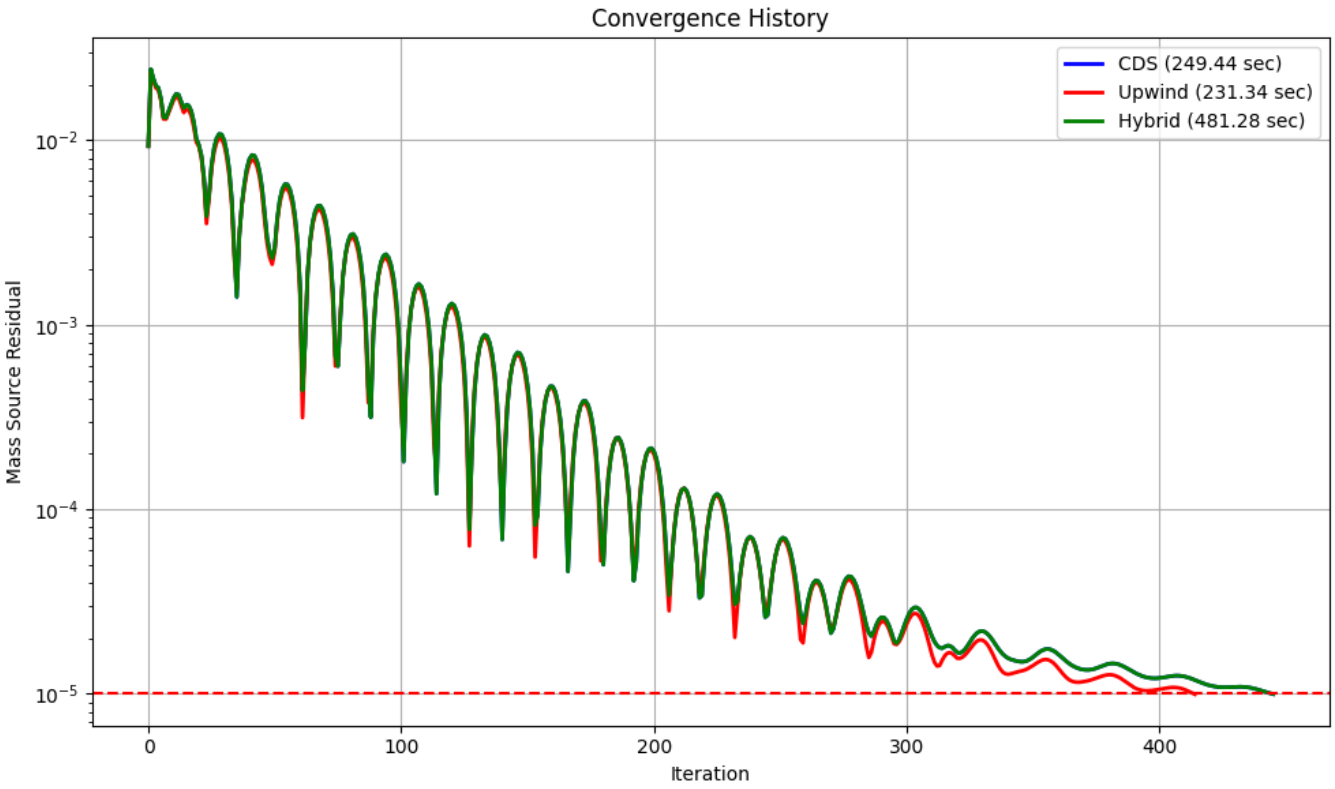

Figure 12: Convergence graph for $\alpha_u = \alpha_v = 0.4$ & $\alpha_p = 0.6$

Very small velocity update (40%) but relatively large pressure update (60%). Slow overall convergence; residual curve shows decent plateau before eventual drop

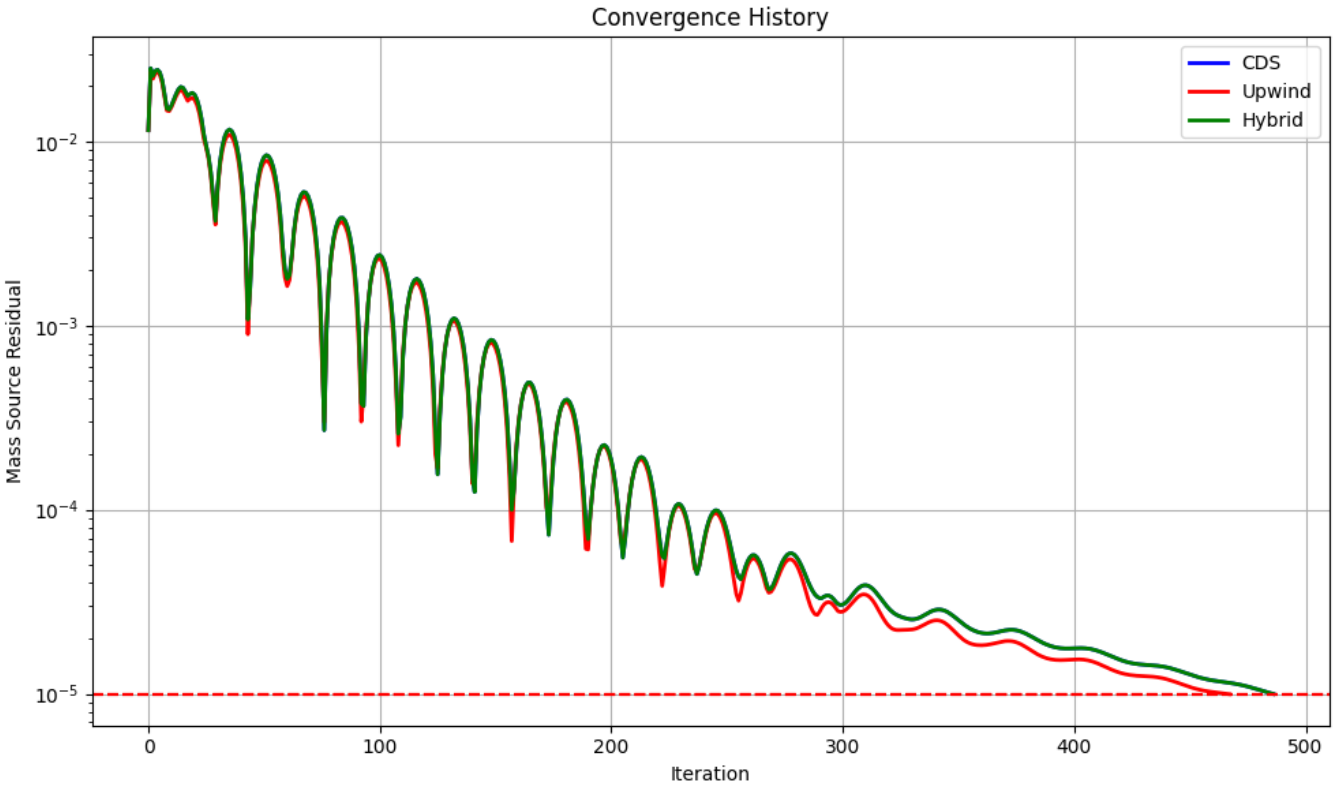

Figure 13: Convergence graph for $\alpha_u = \alpha_v = 0.5$ & $\alpha_p = 0.3$

Moderate velocity update (50%) and conservative pressure update (30%). Marked improvement in convergence stability over previous arrangement, residual drops smoothly. Although iterations increase.

Below is the data for this convergence graph

CDS: Final residual = 9.99198876e-06, Iterations = 487, 236.96 seconds

Upwind: Final residual = 9.96107917e-06, Iterations = 468, 229.59 seconds

Hybrid: Final residual = 9.99198876e-06, Iterations = 487, 236.96 seconds

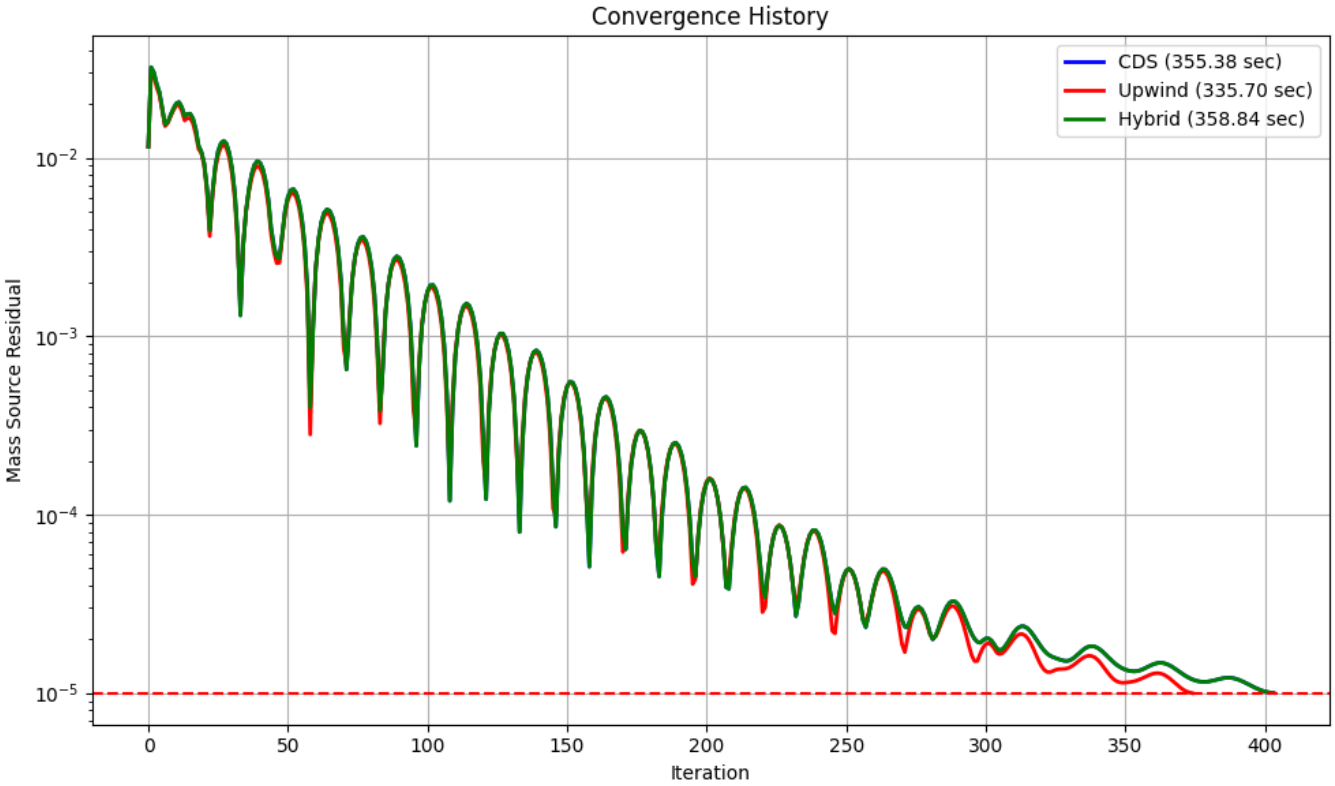

Figure 14: Convergence graph for $\alpha_u = \alpha_v = 0.5$ & $\alpha_p = 0.5$

Equal weighting for velocities and pressure. Converges faster initially than previous arrangement but exhibits small "ripples" in residual before stabilizing.

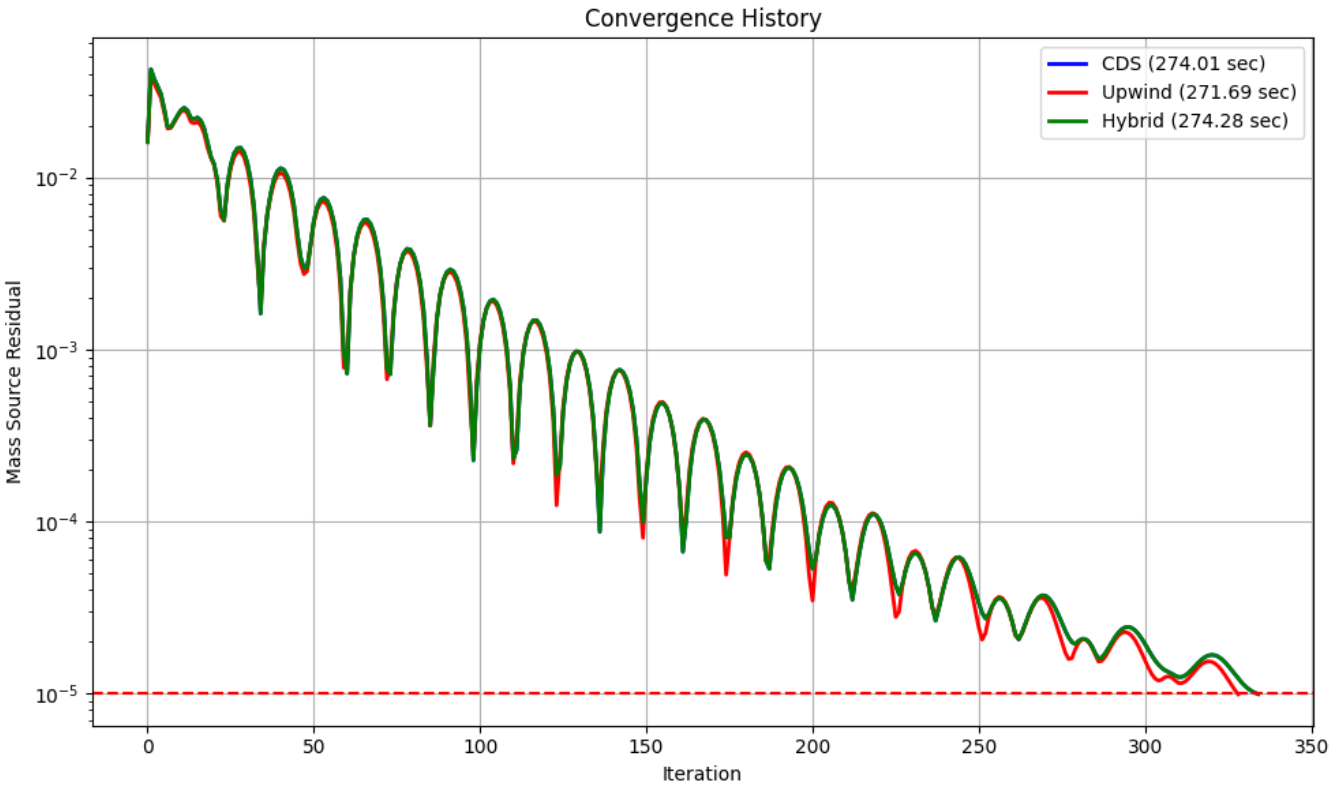

Figure 15: Convergence graph for $\alpha_u = \alpha_v = 0.7$ & $\alpha_p = 0.3$

High velocity update (70%) with cautious pressure update (30%). Pretty fast convergence compared to previous cases. Although the ripples haven't died down fully.

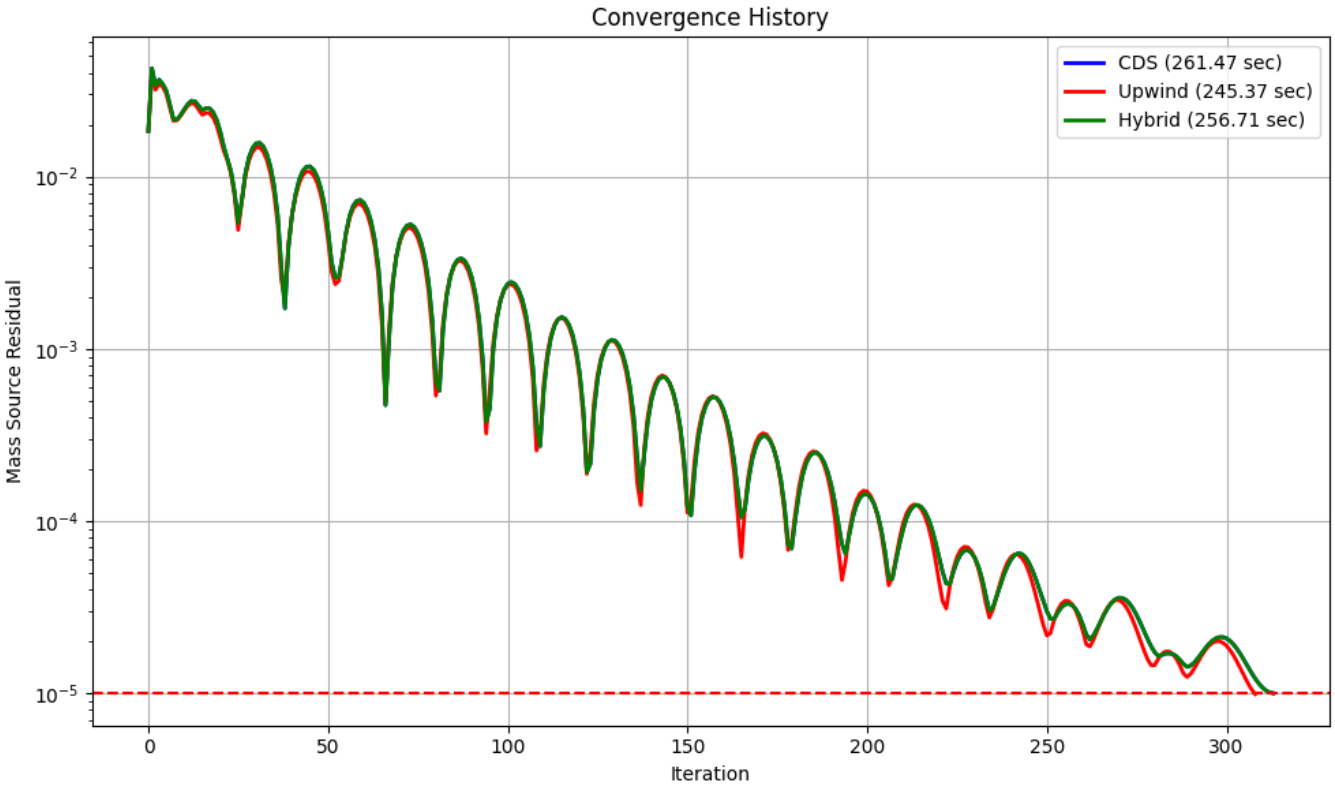

Figure 16: Convergence graph for $\alpha_u = \alpha_v = 0.8$ & $\alpha_p = 0.2$

Very aggressive velocity update (80%) but very damped pressure update (20%). Velocity overshoots can occur because pressure does not correct fast enough to satisfy continuity, leading to slight oscillations. Convergence still faster than moderate cases, but with noticeable small oscillations in the residual curve.

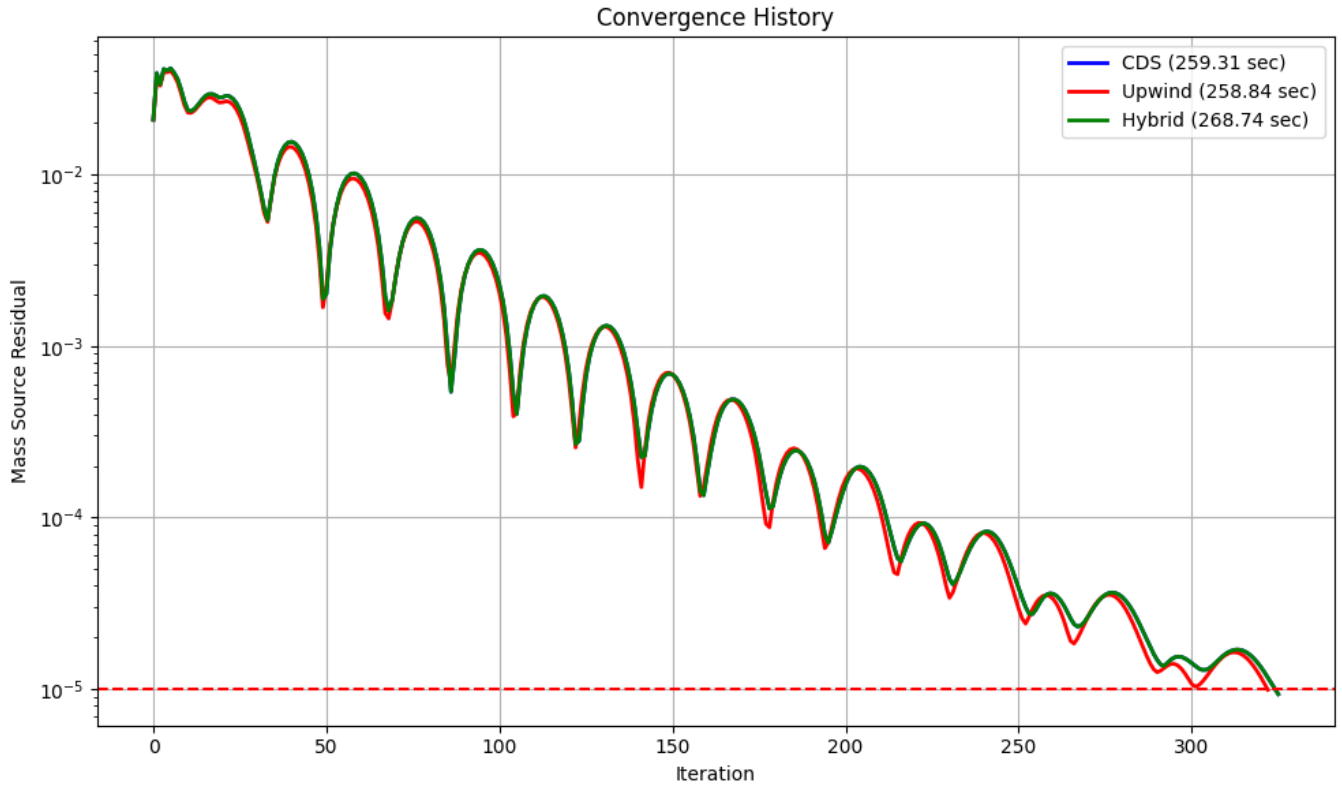

Figure 17: Convergence graph for $\alpha_u = \alpha_v = 0.9$ & $\alpha_p = 0.1$

Extreme velocity updates (90%) paired with minimal pressure correction (10%). Worst performance: residual shows prolonged oscillations. Too-aggressive velocity relaxation without sufficient pressure damping destabilizes the coupling.

5 Conclusion

The numerical solution of the lid-driven cavity flow problem using the Finite Volume Method with the SIMPLE algorithm has been successfully implemented with three different discretization schemes: CDS, Upwind , and Hybrid Scheme. The solution was obtained on a uniform 80x80 cell grid using a staggered grid arrangement. The use of a staggered grid is confirmed to be effective in preventing the checkerboard pressure field issue.

The key findings are:

Discretization Scheme Performance

- The Central Differencing Scheme (CDS) is second-order accurate. However, it is only conditionally stable and may exhibit oscillations, particularly in regions with a high Peclet number. It shows low numerical diffusion and resolves secondary vortices well. Its convergence rate is generally slower compared to Upwind.

- The Upwind Scheme is a first-order accurate scheme and is more stable but introduces numerical diffusion, which can smear the solution. Despite this, Upwind exhibits a faster convergence rate in terms of iterations. The velocity profiles at higher Reynolds numbers (Re=400) highlight the under and over predictive nature of the Upwind scheme. This scheme does not resolve secondary vortices well.
- The Hybrid Scheme combines the advantages of both CDS and UDS, providing a good balance between accuracy and stability. It is described as having first/second-order accuracy, conditional stability, and moderate numerical diffusion. It generally shows a moderate convergence rate and moderately resolves secondary vortices.

Under Relaxation Strategy

- The study also investigated the effect of relaxation factors on the convergence process. Different values for the relaxation factors of velocity (α_u, α_v) and pressure (α_p) result in varying convergence behaviors and computation times, as illustrated by the convergence history graphs.
- Velocity Relaxation ($\alpha_u = \alpha_v$): Increasing from 0.4 to 0.7 steadily accelerates momentum correction without triggering instability; beyond 0.8, residual oscillations emerge.
- Pressure Relaxation (α_p): Values around 0.3 optimally damp pressure-velocity coupling errors; too low (less than 0.1) delays continuity satisfaction, while too high (greater than 0.5) risks checkerboarding.
- Optimal Pair: α_u=$\alpha_v = 0.7$ with $\alpha_p = 0.3$ yields the fastest, smoothest residual decay, cutting iteration counts by up to 50% versus conservative settings

The velocity profiles Re = 100 at the mid-sections of the cavity show differences between the discretization schemes, with CDS generally providing more accurate results in regions of low velocity gradients.

The implementation demonstrates the capability of the Finite Volume Method to accurately capture complex flow phenomena in enclosed cavities, which is relevant to many engineering applications. The choice of discretization scheme depends on the specific requirements of the problem, with a trade-off between accuracy and stability. Although i would suggest that our best bet would be Hybrid scheme with underrelaxation between 0.6 to 0.8 for u and v, 0.3 or 0.4 for p.